KANSAS GEOLOGICAL SURVEY
OPEN-FILE REPORT 2000-45

Statistical Characteristics of Xenoliths in the Antioch Kimberlite Pipe, Marshall County, Northeast Kansas

by

Sergey Kotov
Pieter Berendsen

Disclaimer

The Kansas Geological Survey does not guarantee this document to be free from errors or inaccuracies and disclaims any responsibility or liability for interpretations based on data used in the production of this document or decisions based thereon. This report is intended to make results of research available at the earliest possible date, but is not intended to constitute final or formal publications.

Kansas Geological Survey
1930 Constant Avenue
University of Kansas
Lawrence, KS 66047-3726

Statistical characteristics of xenoliths in the Antioch kimberlite pipe, Marshall County, northeast Kansas.

Sergey Kotov, Pieter Berendsen

Kansas Geological Survey
1930 Constant Avenue
Lawrence, Kansas 66047-3726

Open-file Report No. 2000-45
September 2000

Abstract

Geometrical characteristics of xenoliths in the Antioch kimberlite pipe have been considered in statistical terms. A method of conversion of 2D intersections to 3D dimensions was used. It has been shown that the Rosin-Rammler distribution of mass leads to the Weibull distribution of sizes, while a fractal distribution of sizes can be expressed as the Pareto distribution. Lognormal, Weibull and Pareto distributions have been tested as model distributions. The Pareto distribution could be the most appropriate model for the distribution of xenoliths. This conclusion is in agreement with the general idea that the xenoliths formed as a result of an underground explosion without additional breakage occurring during magma transport. The final distribution may be shifted from the initial model due to processes of redistribution and sorting of xenoliths in liquid-crystalline flows.

Keywords: Lognormal, Weibull, Pareto, fractal, distribution.

Introduction

Investigating processes of xenoliths formation and transport is useful to better understand the internal structure and origination of kimberlite bodies. Different processes of fragmentation lead to different distributions of xenoliths sizes and shapes. Thus, information about sizes and shapes can be used for reconstruction of conditions at which xenolithes formed and for recognizing basic fragmentation processes. Taking into consideration the random character of xenoliths formation we will use some standard statistical procedures for testing model distributions. This approach will allow us not only to choose the appropriate model of breakage but also to estimate the influence of subsequent processes of particles redistribution during magma transport through the kimberlite body which can affect original distributions.

The Antioch kimberlite was selected for this study because two different phases are recognized in the core and the core is competent enough to prepare samples that can be polished for scanning.

The Antioch kimberlite in NWNW section 9, T5S, R8E, Marshall County, is but one of a cluster of twelve identified kimberlites in northern Riley and southern Marshall counties in northeast Kansas. The kimberlites are Late Cretceous in age (about 90 m.y.) and occur along the trace of the 1,10 Ga Central North American Rift System. They intrude into generally flat-lying Permian sedimentary rocks. The top of the Antioch kimberlite is buried beneath 6.5 meters (21 ft.) of alluvial material. The bedrock in the area consists of vari-colored shale and thin limestone units in the upper part of the Council Grove Group, Wolfcampian Series, Lower Permian System (Rotliegendes). Modeling of detailed groundmagnetic data indicates that the Antioch kimberlite is a complex occurrence and should be considered to represent two distinct kimberlite intrusions approximately 150 meters apart (492 ft.). A 95 meter (312 ft.) continuous core was obtained from the northern intrusion. Two distinct rock types can be recognized in the core, probably representing different phases or intrusive pulses. Based on textural and petrographic observations the kimberlite is tentatively classified as diatreme facies.

Assuming that several igneous pulses may be present, the decision was made to see if individual pulses could be statistically recognized based upon the characteristics exhibited by the xenoliths in the core.

Geology

All kimberlites are located in a two-county area in northeast Kansas (Fig. 1) along the NNE-trending trace of the Proterozoic Midcontinent Rift System, an aborted rift extending from the Lake Superior region southwesward into Oklahoma. Three new kimberlites, Antioch, Tuttle, and Baldwin Creek were discovered and drilled in 1999, as part of a systematic ground follow-up of private aeromagnetic data collected by Cominco American in the early 1980's and donated to the Kansas Geological Survey

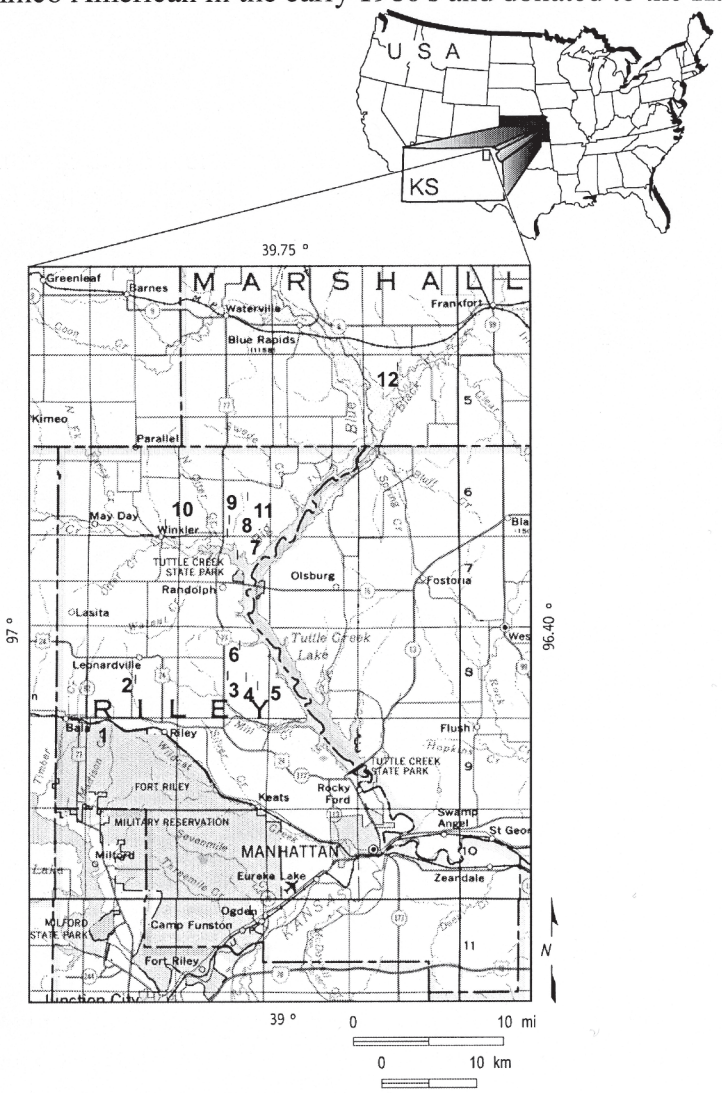

Figure 1. Kimberlite location map. 1. Bala, 2. Leonardville, 3. Tuttle, 4. Lonetree A and B, 5. Stockdale, 6. Baldwin Creek, 7. Fancy Creek, 8. Randolph-1, 9. Randolph-2, 10. Winkler, 11. Swede Creek, 12. Antioch.

in 1999 (Berendsen and Weis, 2000). The kimberlites were drilled to a depth of approximately 92 meters (300 ft.) and continuous core was recovered. The Tuttle and Baldwin Creek kimberlites are in many respects similar in character. The rock has a

light gray-green color in the upper part of the drill hole, turning darker with depth and containing numerous angular to rounded xenoliths of Paleozoic rock fragments and lesser amounts of what are believed to be smaller basement and crustal fragments that are metasomatized to varying degrees. They are both micaceous kimberlites containing garnets and ilmenite up to several centimeters in the Tuttle kimberlite. Secondary gypsum (satin spar), derived from the surrounding Permian redbeds fills fractures up to 4 centimeters (1.6 inches) wide and also occurs as rounded masses up to 4 centimeters (1.6 inches) in diameter.

The Antioch kimberlite occurs 21 km (13 miles) northeast of the cluster of other known kimberlites and is quite different in nature from the other that were drilled. Because the core from this drill hole was used in this study, a brief description of the rock units encountered follows. The kimberlite is overlain by 6.5 meters (21 ft.) of alluvium. Down to 35 meters (115 ft.) the kimberlite is competent, dark-gray-green rock. The matrix is very fine-grained to aphanitic and contains numerous small clasts that are to small to be identified in hand specimens. Occasional, slightly larger clast are to metasomatized to be identified. No garnet, ilmenite, or other minerals can be recognized in the core. At 35 meters (115 ft.) down to 67 meters (115-220 ft.) the kimberlite changes abruptly to a lighter, gray-green, less competent rock containing many larger xenoliths, most of which can be recognized as being pieces of the local Paleozoic sedimentary section. From 67-71 meters (220-233 ft.) the kimberlite looks very similar to that in the upper part of the core. At 71 meters (233 ft.) down to 81 meters (266 ft.) another sharp change to lighter-colored and less competent kimberlite occurs. The last 13 meters (43 ft.) consists again of dark gray, fine grained, and competent kimberlite. Based on textural and petrograhic observations the kimberlite is tentatively classified as diatreme facies.

The tectonic setting in northeast Kansas is just right for accommodating the intrusion of kimberlites. The major structural elements are the regional NNE-trending, deep-seated, high-angle normal and reverse faults associated with the 1.10 Ga Midcontinent Rift System and the regional, older, high-angle normal and reverse, NW-SE striking,crosscutting faults which offset portions of the rift (Berendsen and Blair, 1986). The presence of the rift is identified in regional gravity (Coons et al, 1967) and magnetic data (King and Zietz, 1971) sets and evidenced in core and cuttings recovered from drill holes that penetrate the Precambrian basement. In the area where the kimberlites occur the rift cuts through metamorphic and granitoid rocks of the Central Plains orogen, ranging in age from 1.63-1.80 Ga (Sims and Peterman, 1986; Bickford et al, 1981).

Sample processing.

Samples from kimberlite core were cut and polished. Scanned images were processed using Adobe Photoshop for image enhancement (adjustment of brightness, contrast and noise removal). The recognition and measurement of xenoliths was conducted using UTHSCSA ImageTool – a freely distributed image processing and analysis program. Xenoliths were isolated using thresholding of grayscale images followed by measuring different features of xenoliths such as length of main axes, elongation,

roundness ((4 x Pi x area) / perimeter^2), compactness (sqrt(4 x area / Pi) / major axis length), Feret diameter of xenoliths (the diameter of a circle having the same area as the object = sqrt(4 x area) / Pi) etc.

Conversion of 2D intersections to 3D dimensions.

The raw data on xenolith sizes represent only a measurement of intersections of xenoliths with a plane. Conversion of two-dimensional size to true three-dimensional size distribution is a stereological problem (see Royet, 1991). There are two main problems: a so called cut effect and an intersection effect. The cut effect concerns the reduction in intersection sizes due to the random intersection of the xenolith with the plane which does not necessarily pass directly through the center of xenolith. For a set of xenoliths with different sizes, smaller xenoliths are less likely to be intersected by a plane than larger xenoliths. This is the intersection-probability effect. Review of possible solutions of these problems can be found in Higgins (2000). In this research, we used a method proposed by Saltykov (1967), and further developed in Sahagian and Proussevitch (1998). According to this method, the raw data have to be sorted into m geometrical size classes. The number of classes was defined as $m \approx \lg_2(n)$, where n is a number of xenoliths in raw data. This is necessary for the correct Chi-squared statistical testing of the resulting distributions. In our case we used classes each $10^{-0.1}$ smaller than the last (bigger xenoliths fall into bigger size classes). The true number of xenoliths N_{Vi} that fall into the i-th size class can be estimated then as follows:

$$N_{V_1} = \frac{N_{A_1}}{P_{11} H_1}, \qquad N_{V_i} = \frac{N_{A_i} - \sum_{j=1}^{i-1} N_{V_j} H_j P_{ji}}{P_{ii} H_i}. \qquad (1)$$

Here N_{Ai} is a number of xenoliths from the i-th class of raw data obtained from a section. H_i is the Mean Projected Height which can be defined as the mean height of the shadow of the xenolith from i-th size class for all possible orientations (Sahagian and Proussevitch, 1998). H_i provide intersection effect correction. P_{ji} is the probability that a xenolith with a true size in the class j will have an intersection that falls in the class i (correction of the cut-section effect). A simple solution for estimation of H_i and P_{ji} for a set of xenoliths with different sizes and shapes does not exist. Possible approaches using random simulation of xenoliths with known shapes are discussed in Higgins (2000) and Sahagian and Proussevitch (1998). In this research we used a spherical model of xenoliths which allows the simple analytical solution. In this case H_i is simply a mean diameter of xenoliths in class i and P_{ji} can be obtained from the equation $P_{ji} = \frac{1}{H_j}\left(\sqrt{H_j^2 - r_{i+1}^2} - \sqrt{H_j^2 - r_i^2}\right)$, where r_{i+1} and r_i are maximum and minimum values in the class i. In addition, the resulting values N_{Vi} were renormalized so as their sum would be equal to the total number of measured xenoliths. The last step provides the invariance of results relative to units of measurement.

Some theoretical models of breakage.

1. In 1941 Kolmogorov and in 1947 Epstein investigated the breakage process using the following assumptions: fragmentation can be considered as composed of discrete steps of breakage events, the probability of breakage of any piece during any step of process is constant, the distribution of pieces obtained from the application of a single breakage event to a given piece is independent of the dimension of the piece broken (Epstein, 1947). It was shown that under these assumptions, any initial fragment distribution eventually tends toward a log-normal distribution of the form

$$P\{l < x\} = F(x) = \frac{1}{2}(1 + erf(\frac{\ln x - \ln a}{\sigma\sqrt{2}})). \qquad (2)$$

$P\{l < x\}$ is a probability of a xenolith size l to be less then x.
The density function is

$$f(x) = \frac{1}{\sqrt{2\pi}\sigma x}\exp(\frac{-(\ln x - \ln a)^2}{2\sigma^2}). \qquad (3)$$

Estimations of parameters of the distribution can be obtained from a sample as follows:

$$\sigma = \sqrt{\ln(\frac{s^2}{x_a^2} + 1)}; \quad a = x_a \exp(-\frac{1}{2}\sigma^2). \qquad (4)$$

where x_a and s are an average sample value and standard deviation respectively.

2. Commercial crushing and grinding processes generally produce a Rosin-Rammler distribution of the form

$$\frac{N(m)}{N_T} = \exp\left(-\frac{m}{\mu}\right)^{\upsilon}, \qquad (5)$$

$N(m)$ is the number of fragments with a mass greater than m, N_T is the total number of fragments, μ, ν are free parameters.

This distribution results when comminution is controlled by a Poisson distribution of initial flaw sizes in the starting material (Gilvarry and Bergstrom, 1961).

Unfortunately, in this form the distribution is not appropriate for statistical testing. Moreover, this distribution is a function of fragment masses, whereas we need the distribution of sizes. Let us conduct some simple transformations. In statistical terms $\frac{N(m)}{N_T} \xrightarrow[N_T \to \infty]{} P\{m > x\}; x > 0$. Consequently $P\{m < x\} = F_m(x) = 1 - \exp\left(-\frac{x}{\mu}\right)^{\upsilon}$.
But this is the Weibull distribution with free parameters μ and ν.

Our final interest is a distribution of sizes r. Let us express the mass of a xenolith as $m=r^3c$, where $c=s\rho$. Here ρ is density of a substance, s is a positive shape constant (for

example $s=4/3\pi$ for a sphere). $r=f(m)=(m/c)^{1/3}$ is a monotonously increasing function of m. Hence, it is possible to write the distribution function $F_r(x)$ as follows:

$$F_r(x) = P\{f(m) < x\} = P\{m < f^{-1}(x)\} = F_r(f^{-1}(x)),\ \text{i.e.}\ F_r(x) = 1 - \exp\left(-\left(\frac{x^3 c}{\mu}\right)^{\upsilon}\right).$$

Using substitution $\beta = (\mu/c)^{1/3}, \alpha = 3\upsilon$ we easily obtain the $F_r(x) = 1 - \exp\left(-\frac{x}{\beta}\right)^{\alpha}$.

This is again the Weibull distribution with some parameters α and β. The density function is $f_r(x) = \alpha\beta^{-\alpha}x^{\alpha-1}\exp(-(x/\beta)^{\alpha})$. Unfortunately, there exists no simple way for estimation of the parameters from a sample. In this article we use the α=1 and $\beta=x_a$ as a starting approximation with the consequent search of a point in the parametrical space minimizing the Chi-squared function (see explanations below).

3. One more distribution we will use here is the fractal distribution. As it was shown in Sammis and Steacy (1995), this distribution law can arise when fracturing has place in constrained conditions when fragments are not free to change their relative positions. This conditions can be produced by underground explosions, in some fault zones etc. (see e.g. Turcotte, 1986). Most often this law is written as follows: $N(r) \propto r^{-D}$ where N is the number of xenoliths with size more than r. Again, this form of distribution allows to test this dependence on qualitative level and estimate D – fractal dimension, but it does not allow the statistical testing of the distribution. The necessary transformations are as follows:

$\frac{N(r)}{N_T} \xrightarrow[N_T \to \infty]{} P\{r > x\}$, where $P\{r > x\}$ is the probability that a randomly chosen xenolith has a size more than x. Consequently $P\{r < x\} = F_r(x) = 1 - Cx^{-D}$, where C is some constant. To define the distribution function entirely we have to choose the C so as the integral of the density function $f_r(x) = CDx^{-D-1}$ over the function's support be 1. It is possible to do for the interval $[\Delta,\infty]$ where Δ is any positive number. In this case $C=\Delta^D$. So, the resulting distribution function is $F_r(x) = 1 - \left(\frac{\Delta}{x}\right)^D$ and the density function is $f_r(x) = Dx^{-D-1}\Delta^D$. This is nothing else but the Pareto distribution with the parameter D. The unbiased estimation of D is $\hat{D} = 1/2 + \sqrt{1/4 + \Delta/x_a}$ where Δ can be defined as a minimum value from the empirical sample and x_a is an average value of the sample.

Thus, in this article we consider three distribution functions (log-normal, Weibull and Pareto) as possible models of breakage process. Testing of distributions was conducted using standard Chi-squared technique. That is to say, the value

$\chi_n^2 = \sum_{i=1}^{m} \frac{(n_i - np_i(\theta))^2}{np_i(\theta)}$ was used as a measure of a difference between theoretical and empirical distributions. Here, n_i is a number of xenoliths in the i-th bin of histogram,

m is a number of bins, $p_i(\theta)$ defines the probability of random xenolith to fall into i-th bin:

$p_i(\theta) = \int_{x_i}^{x_{i+1}} p(x,\theta)dx$, where $p(x,\theta)$ is a density function for chosen distribution, x_i and x_{i+1} are margins of i-th bin. At big values of n, χ_n^2 converges to the χ^2 distribution with m-k-1 degrees of freedom, where k is the number of parameters of model distribution. The vector of parameters θ was chosen so as to minimize the Chi-squared function. This was provided by the substitution of unbiased estimations of parameters (excluding Weibull distribution, see above) followed by a simple coordinate descent in the parametrical space.

The use of distance between the theoretical and empiricals distribution allows us not only to test a distribution (accept or reject a model with chosen reliability) but also to estimate the measure of influence of additional processes disturbing the original distribution. In our case, deviations from the supposed theoretical distributions can be explained by mixing of several kimberlite magmas with different sources of xenoliths or by redistribution of xenoliths during transport of magma through the kimberlite pipe.

Discussion of results.

An average length, perimeter, area, Feret diameter reflect the overall size of xenoliths and, consequently, they are highly correlated. It is possible to note the tendency of increasing average size with depth (fig. 2).

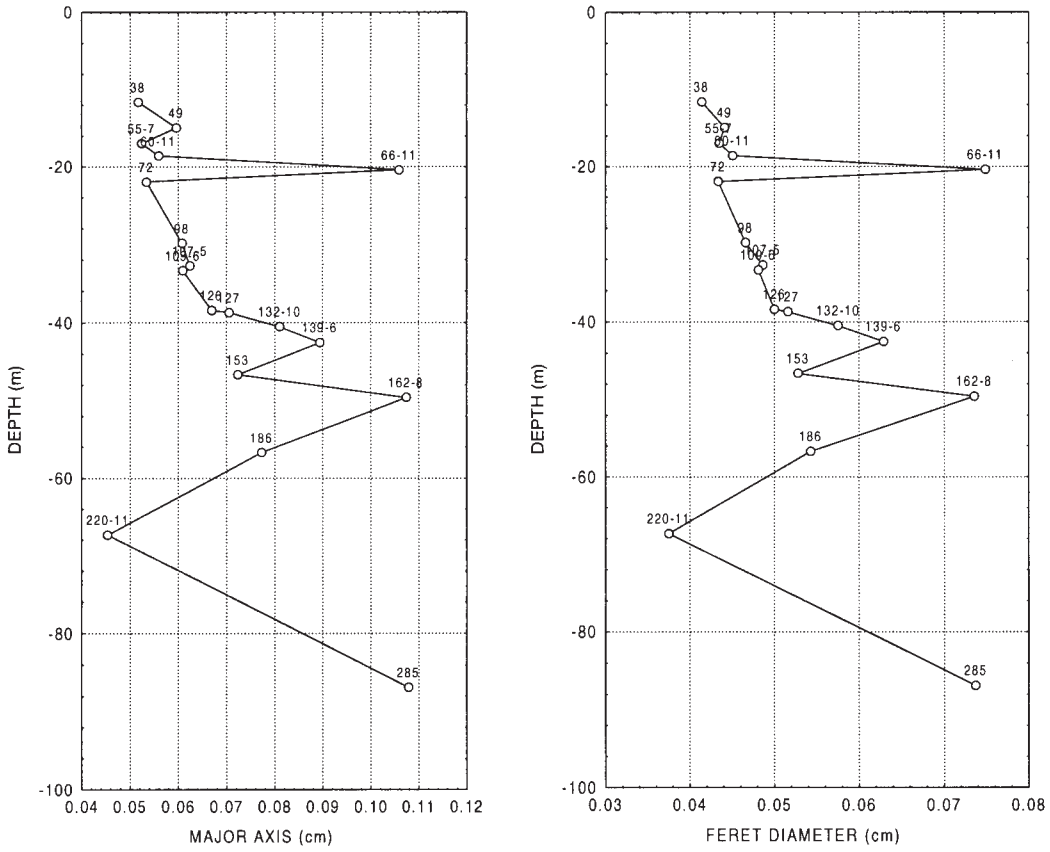

Figure 2. An average length of major axis and Feret diameter of xenoliths with depth.

This tendency is sporadically disturbed by sudden changes of average values, which can be explained by the presence of additional magmatic sources (samples 66-11, 162-8, 220-11). The same tendency has the distribution of elongation, whereas the compactness and roundness are described by the inverse dependence (fig. 3). This is expressed also in significant coefficients of correlation between the length of major axis and elongation (r = 0.87), Feret diameter and elongation (r = 0.83), major axis and roundness (r = -0.92), major axis and compactness (r = -0.91), Feret diameter and roundness (r = -0.88), Feret diameter and compactness (r = -0.88).

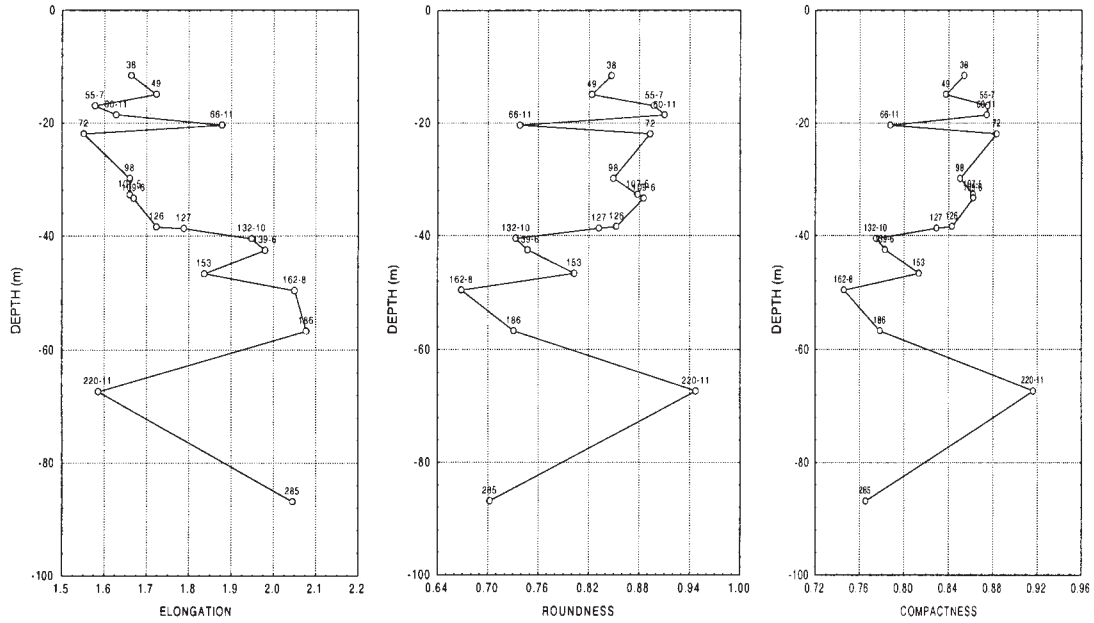

Figure 3. Elongation, roundness and compactness versus depth.

Thus, an average isometricity of xenoliths decreases with their size.

Results of testing of corrected distributions of sizes on correspondence with model laws of distributions are follows:

1. Logarithmic and Weibull distributions are rejected for all samples with reliability 99%.
2. The most adequate model, describing empirical distributions, is the fractal distribution (Pareto distribution in our terminology). This conclusion is in the agreement with the idea of xenolith formation as a result of rocks exploding under constrained conditions at depths. Almost one half of the samples does not statistically contradict to Pareto distribution. The rest of the samples is characterized by distributions of sizes that are slightly shifted from the model distribution. Although these shifts are not as large as for lognormal and Weibull distributions, they are sufficient enough for the Pareto distribution to be rejected. These shifts can be attributed to the xenoliths redistribution due to mixing of different magmatic fractions or to the redistribution of xenoliths during transport of magma through a kimberlite pipe.

Tabl. 1. Estimation of Chi-squared values and critical Chi-squared values for lognormal, Weibull and Pareto distributions. A distribution is rejected with the reliability 99% if the estimation exceeds the critical value.

Sample N	Lognormal distr.	Weibull distr.	Critical values	Pareto distr.	Critical values
38	123	637	18.5	73	20.1
49	18762	54	16.8	1	18.5
55-7	168	713	18.5	58	20.1
60-11	126	526	18.5	26	20.1
66-11	92	381	18.5	10	20.1
72	248	1054	18.5	20	20.1

98	143	611	20.1	41	21.7
107-5	52	234	16.8	10	18.5
109-6	176	802	18.5	32	20.1
126	103	467	18.5	8	20.1
127	226	897	18.5	9	20.1
132-10	80	360	18.5	35	20.1
139-6	74	340	16.8	15	18.5
153	120	551	18.5	26	20.1
162-8	42	241	18.5	20	20.1
186	70	300	18.5	32	20.1
220-11	1399	1539	20.1	34	21.7
285	44	266	18.5	34	20.1

This is possible, for example, due to the Bagnold effect, according to which xenoliths can be sorted by size during transportation of liquid-crystalline flows, even recovering effects of gravitational layering (Hutter, 1993).

The distribution of Chi-squared estimations are shown in the figure 4.

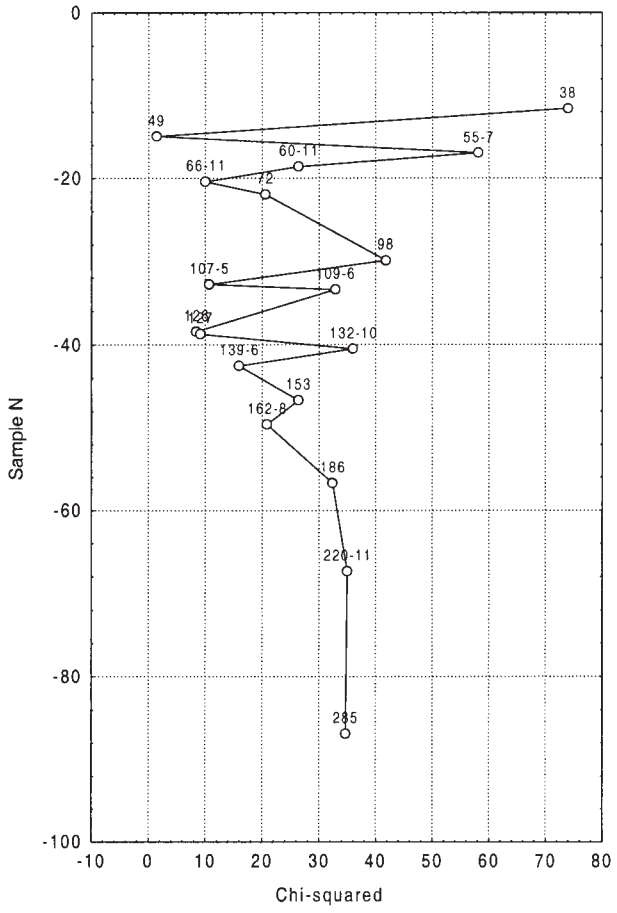

Figure 4. Chi-squared estimations and critical chi-squared values for Pareto distribution.

Chi-squared values do not correlate with any shape and size characteristics of xenoliths. This means that processes of redistribution and sorting of xenoliths occurred independently in different parts of kimberlite body. But it is possible to note that these processes were developed more intensively in the upper part of the pipe.

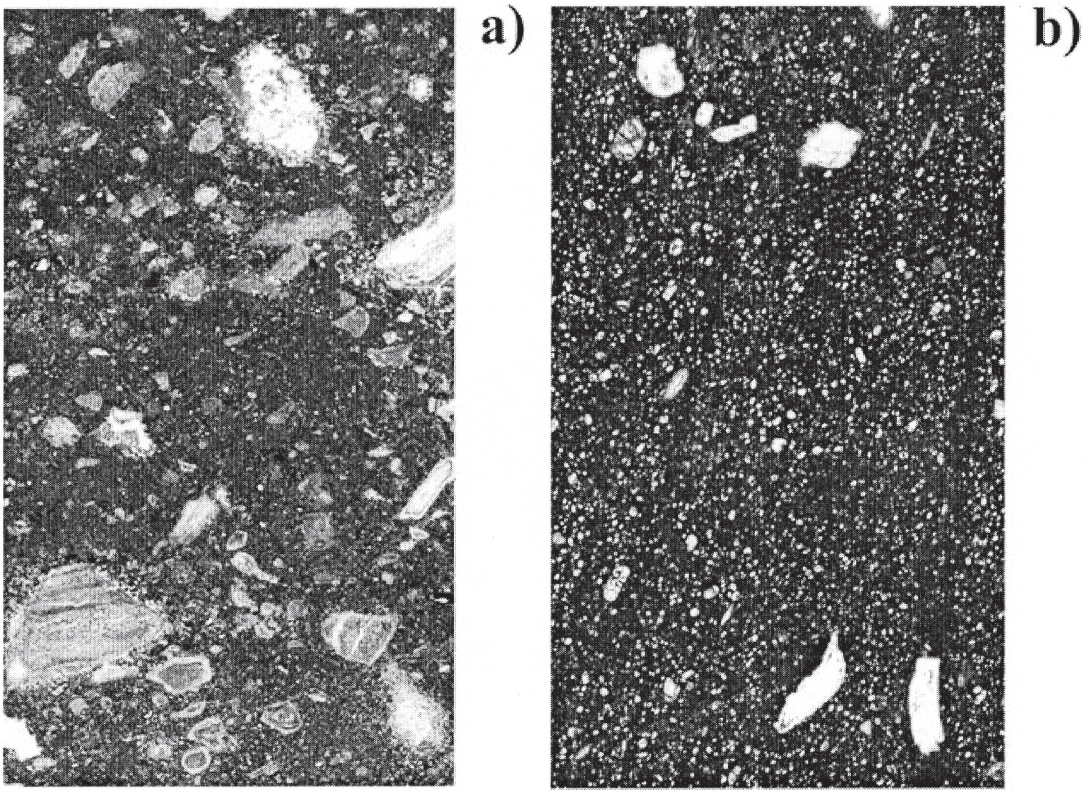

Figure 5. Character of typical xenoliths distribution in the Antioch kimberlite pipe: a) sample 66-11; b) sample 220-11. See discussion in text.

Figure 5 illustrates typical distributions of xenoliths in the pipe. The distribution of sizes in the sample 66-11 does not contradict to the fractal (Pareto) distribution. For the sample 220-11 all considered models of distributions are rejected with the reliability 99%. One can see distinct prevalence of xenoliths with smaller sizes. Moreover, careful examination allows to see sub-vertical traces of viscous flows of liquid-crystalline mass. Possibly, these flows were the cause of a distribution shift from the theoretical model.

Thus, by examining the statistical characteristics of xenoliths it is possible to propose that the examined section of the Antioch kimberlite pipe consists of a main body with increase of the mean xenoliths size and decrease of xenoliths isometricity with depth. This body was disturbed by additional portions of magma with a different source of xenoliths. Probably, all xenoliths were formed as a result of an underground explosion without additional processes of fragmentation during the transport stage. All magmas was slightly influenced by processes of redistribution and sorting of xenoliths during magma transport through the kimberlite pipe.

References.

Berendsen, P., and Blair, K. P. (1986), Tectonic evolution of the Midcontinent Rift System in Kansas // Geological Society of America Special Paper 312, pp. 235 – 141.

Berendsen, P., and Weis, T (2000) New kimberlite discoveries in Kansas, what do they tell us about the Precambrian basement in the mid-continent, U.S.A.: Variscan-Appalachian dynamics: the building of the Upper Paleozoic basement. Basement Tectonics 15, A CoruЯa, Spain, Program and Abstracts, 7, pp. 61 – 62.

Bickford, M. E., Harrower, K. L., Hoppe, J. W., Nelson, B. K., Nusbaum, R. L., and Thomas, J. J. (1981) Rb-Sr and U-Pb geochronology and distribution of rock types in the Precambrian basement of Missouri and Kansas // Geological Society of America Bulletin, part 1, v. 92, pp. 323 – 341.

Coons, R. L., Woollard, G. P., and Hershey, G (1967) Structural significance and analysis of Midcontinent Gravity High // American Association Petroleum Geologists Bulletin, v. 51, no. 12, pp. 2381 – 2399.

Epstein B.J. (1947) The Mathematical Description of Certain Breakage Mechanisms Leading to the Logarithmico-Normal Distribution // Franclin Inst., v. 244, pp. 471 – 477.

Gilvarry J.J. and Bergstrom B.H. (1961) Fracture of Brittle Solids. II. Distribution Function for Fragment Size in Single Fracture (Experimental) // J. Appl. Phys., 32, pp. 400 – 410.

Higgins M.D. (2000) Measurement of Crystal Size Distributions. // American Mineralogist, v.85

Hutter K., editor. (1993) Continuum Mechanics in Environmental Sciences and Geophysics. Springer-Verlag: Wien-New York, 522 p.

King, E. R., and Zietz, I. (1971) Aeromagnetic study of the Midcontinent Gravity High of central United States: Geological Society of America Bulletin, v. 82, pp. 2187-2208.

Kolmogorov A.N. (1941) The Lognormal Law of Distribution of Particle Sizes during crushing // Dokl. Akad. Sci. USSR, v.31 (2), pp. 99 – 101.

Royet, J.P. (1991) Stereology: A Method for Analysing Images. // Progress in Neurobiology, 37, pp. 433 – 474.

Sahagian D.L., Proussevitch A.A. (1998) 3D Xenolith Size Distributions from Natural Applications. // Journal of Volcanology and Geothermal Research, v.84, pp.173 –196.

Saltikov S.A. (1967) The Determination of the Size Distribution of Xenoliths in an Opaque Material from a Measurement of the Size Distributions of Their Sections. In

H. Elias, Ed. Proceedings of the Second International Congress for Stereology. Springer-Verlag: Berlin, pp. 163 – 173.

Sammis C.G., Steacy S.J. (1995) Fractal Fragmentation in Crustal Shear Zones // in "Fractals in the Earth Sciences." Ed. by Barton C.C. and La Pointe P.R. pp. 179 – 204.

Sims, P. K., and Peterman, Z. E. (1986) Early Proterozoic Central Plains orogen: a major buried structure in the north-central United States: Geology, v.14, pp. 488 – 491.

Turcotte D.L. (1986) Fractals and Fragmentation // J. Geophys. Res., v.91, pp.1921 – 1926.